Optimal Design of a Squeeze Film Damper Using an Enhanced Genetic Algorithm

Young Kong Ahn, Young-Chan Kim, Bo-Suk Yang*
School of Mechanical Engineering, Pukyong National University, San 100, Yongdang-dong, Nam-gu, Busan 608-739, Korea

This paper represents that an enhanced genetic algorithm (EGA) is applied to optimal design of a squeeze film damper (SFD) to minimize the maximum transmitted load between the bearing and foundation in the operational speed range. A general genetic algorithm (GA) is well known as a useful global optimization technique for complex and nonlinear optimization problems. The EGA consists of the GA to optimize multi-modal functions and the simplex method to search intensively the candidate solutions by the GA for optimal solutions. The performance of the EGA with a benchmark function is compared to them by the IGA (Immune-Genetic Algorithm) and SQP (Sequential Quadratic Programming). The radius, length and radial clearance of the SFD are defined as the design parameters. The objective function is the minimization of a maximum transmitted load of a flexible rotor system with the nonlinear SFDs in the operating speed range. The effectiveness of the EGA for the optimal design of the SFD is discussed from a numerical example.

Key Words: Squeeze Film Damper, Genetic Algorithm, Optimum Design, Rotor Dynamics, Global Optimization

1. Introduction

A squeeze film damper (SFD) consists of a rolling element bearing, cylindrical journal and centering spring to support a shaft, which adds externally additional damping to flexible rotor systems (Thomsen and Andersen, 1974; Satio and Kobayashi, 1982; Cunningham et al., 1975). When designing the SFD, its shape and oil viscosity used in a SFD can be varied in order to obtain the optimum support damping at an operational speed. Several authors (Thomsen and Andersen, 1974; Satio and Kobayashi, 1982; Cunningham et al., 1975; Ahn et al. 1998) pointed out that the optimum support damping introduced by the SFD depends on whirling modes of the rotor.

Since high-speed rotating machinery such as aircraft engines, generators and compressors are usually supported on a rolling element bearing which offer very little damping, some squeeze film dampers are employed to reduce the unbalance response, particularly at critical speeds. In the design of modern machinery, the rotors require light-weight and high-performance, which usually lead to more flexible and complex assembles and to more difficulty with design problems. Several publications represented the design methodology for sizing nonlinear SFDs (Gunter et al., 1977; Rabinowitz and Hahn, 1983; Mohan and Hahn, 1974; Chen et al., 1988; Lin et al., 1998; Shiau et al., 1993), while they had the absence of a nonlinear behavior of the SFD (Lubell and San Andres, 1998; De Santiago et al., 1999). Especially, Chen et al.(1988) first addressed the design of the nonlinear SFD by using an automated optimization technique which is a nonlinear

* Corresponding Author,
E-mail: bsyang@pknu.ac.kr
TEL: +82-51-620-1604; **FAX**: +82-51-620-1405
School of Mechanical Engineering, Pukyong National University, San 100, Yongdang-dong, Nam-gu, Busan 608-739, Korea. (Manuscript **Received** March 2, 2002; **Revised** September 27, 2003)

programming (NLP) technique for the minimum transmitted force to the bearing and foundation in the operational speed range. Since the search by the NLP technique tends to converge into an unstable solution according to the initial design values, the design iteration needs to be repeated with a different set of initial system parameters when the obtained solution may not be a global optimum.

In general, it is not easy to solve such a nonlinear objective function by local optimization techniques. Many optimization techniques for the nonlinear objective function have been proposed, and maybe the genetic algorithm among the techniques is most well known as a global optimization technique. The genetic algorithm has recently received considerable attention regarding its capability as an optimization technique for complex and linear optimization problems, and successfully applied to several engineering algorithms. However, a general GA can not optimize multi-modal functions.

In this study, the enhanced genetic algorithm (EGA) (Kim et al., 2001) proposed to optimize multi-modal functions is applied to the minimization of the maximum transmitted load of a rotor system with the nonlinear SFDs between the bearing and foundation in the operating speed range. The radius, length and clearance of the SFDs are chosen as the damper design parameters. The EGA consists of the GA and the simplex method. When the GA to search global and local optimal solutions is combined with the simplex method to search intensively the candidate solutions by the GA for the optimal solutions, the searching time of the hybrid algorithm decreased and the accuracy of the solutions increased compared with the IGA (Immune-Genetic Algorithm) (Choi and Yang, 2001) for the multi-modal function optimizations. Furthermore, the advantage of this algorithm is that any kind of objective functions can converge into a stable solution and does not need to use design sensitivity analysis for an optimum problem. The SQP (Sequential Quadratic Programming) (The Mathworks Inc.) is more quickly converged into a solution than the EGA and IGA but is not able to find global optimum solutions according to an initial value.

A numerical study represents that the maximum transmitted load of the flexible rotor system with the SFDs optimized by the EGA was remarkably reduced and also done more than that by Chen et al. (1988).

2. Enhanced Genetic Algorithm (EGA)

A general genetic algorithm (GA) was described by Goldberg (1989) and Davis (1991), which is able to search only global optimum solutions by estimating fitness of individuals, but not able to optimize multi-modal functions. The search by the GA is not in need of much mathematical requirements about optimization problems due to its evolutionary property. Furthermore, the GA can handle any kind of objective functions defined as a linear or nonlinear function with any kind of constraints. The GA has more flexible and faster convergence characteristics than a single point search method because this algorithm can define the objective function with a multitude of design parameters (Okamoto et al., 1998 ; Merz and Freisleben, 2000 ; Choi and Yang, 2000). Recently, new hybrid GAs to search optimum solutions of multi-modal functions and to increase the accuracy of optimum solutions were proposed (Sato and Hagiwara, 1998 ; Choi and Yang, 2001).

The EGA consists of the GA and the simplex method (Kim et al., 2001). The local and global optimal solutions can be searched by the GA, and furthermore, the simplex method (Nelder and Mead, 1965) is combined with the GA to increase the accuracy of the solutions. Moreover, the searching time by the hybrid algorithm with the simplex method is decreased consequently in comparison with the conventional GA. The EGA has two main processes, one process is to search globally optimal solutions and the another is to search locally candidate solutions by the GA for optimal solutions. The flow chart of the EGA shown in Figure 1 is as follows.

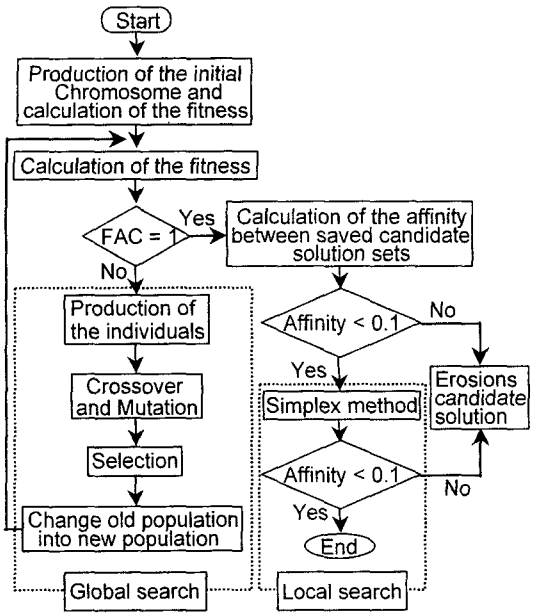

Fig. 1 The flow chart of the EGA

Step 1. Production of the initial chromosome : The genetic uniform distribution method is used to prevent the search converging to a local optimum.

Step 2. Calculation of the fitness and affinity of individuals : The affinity evaluation function (AEF) which estimates the affinity among the groups of initial candidate solutions, is defined as

$$AEF_{i,j}=\frac{\sum_{i}^{N-1}\sum_{j=i+1}^{N}(x_i-x_j)}{Norm(\boldsymbol{x})}, \qquad \boldsymbol{ac}_{i,j}=\begin{cases}1 : AEF_{i,j}\leq T_a \text{ or } i\geq j\\ 0 : otherwise\end{cases} \tag{1}$$

where the vector $\boldsymbol{x}$ is the total candidate solutions which were selected in the global search step, T_a is the threshold value of the AEF, and $\boldsymbol{ac}_{i,j}$ is the square matrix which consists of values between 0 and 1. The subscript i and j means that the j-th solution is compared with the i-th solution. In this paper, 0.1 is used as T_a. N is the integer number of the initial candidate solutions, which must be set large enough to search all optimum solutions. The proposed N is as follows :

$$N\geq\frac{3N_i}{FAC}+\frac{1-FAC}{0.1\times FAC} \tag{2}$$

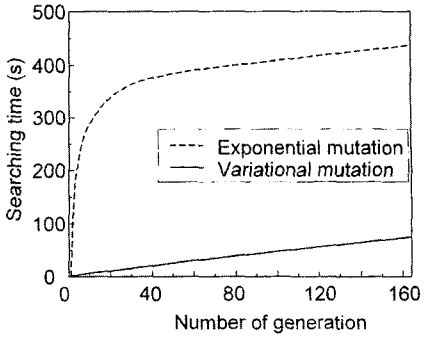

Fig. 2 Comparison of the searching time between the exponential and variational mutation ratios

where N_i is the number of the optimum solutions determined by the EGA. The functional assurance criterion (FAC) (Friswell and Mottershead, 1996) is defined as follow :

$$FAC=\frac{|\boldsymbol{f}_{i-1}^T\boldsymbol{f}_i|^2}{(\boldsymbol{f}_{i-1}^T\boldsymbol{f}_{i-1})(\boldsymbol{f}_i^T\boldsymbol{f}_i)} \tag{3}$$

where the row vector $\boldsymbol{f}_i$ is defined by the fitness values of the individuals at the ith generation and $\boldsymbol{f}^T$ means the transpose of $\boldsymbol{f}$. the size of the vector $\boldsymbol{f}$ depends on the number of the optimum solutions. Theoretically, the range of the FAC is between 0 and 1. When the value of the FAC is selected as 1, this algorithm searches only the global optimum solutions.

Step 3. Production of the individual, and crossover and mutation : In producing individuals, the genetic uniform distribution method and the variational mutation are used to improve the efficiency of the global search. The mutation which is one of the most important operators of the GA prevents early the search from converging into local optimal solutions. When a high mutation rate is selected, the good genes of parents are easily lost. Then, it is difficult for the individuals to satisfy the constraint conditions. Figure 2 shows the comparison of the searching time between the exponential and variational mutation ratios according to the increase in the generation number. An example quoted from reference (Hashimoto, 1997) is used in the investigation of the efficiency of the mutation rate. Searching time in the case of the exponential

mutation greatly increases more than one in that of the variational mutation.

Step 4. Estimation and production of the initial solutions by constraint conditions and parameter range.

Step 5. Selection of the candidate solutions by using the FAC.

Step 6. Deciding the similarity among candidate solutions.

Step 7. Searching the optimum solutions by the simplex method on each candidate (intensive local search): The candidates obtained by the global search are used in the local search. The simplex method in the local search process intensively searches the candidate solutions for the optimal solutions.

Step 8. Deciding the final optimum solutions.

The performance of the EGA with a benchmark function is compared to them by the IGA and SQP of the local optimization technique which is well known as the NLP technique. The optimization results are shown in Table 1 and the benchmark function to test the optimization algorithms (De Jong, 1975) is as follows:

$$f(x_1, x_2) = (\cos 2\pi x_1 + \cos 2.5\pi x_1 - 2.1)(2.1 - \cos 3\pi x^2 - \cos 3.5\pi x_2) \quad (4)$$
$$(-1.0 \le x_1, x_2 \le 1.0)$$

Eq. (4) which is a multi-modal function has four local optimums of $f(x) = 14.333087$, and four global optimums of $f(x) = 16.091720$. The EGA and IGA searched all global optimum solutions. However, the EGA obtained more accurate optimum solutions than the IGA, and the searching time of the EGA is twenty times faster than that of the IGA. Although the EGA generally takes more running time than a general GA which can not optimize multi-modal functions, it obtains more accurate solutions than a general GA. However, the optimization techniques offer a trade-off between running time and solution accuracy. The SQP was more quickly converged into a solution than the other algorithms but was not able to find global optimum solutions from the initial value. The searching time and solution accuracy by Chen et al.(1988) could not be compared with them by the EGA because them by Chen et al.(1988) were not represented in their article.

Table 1 Comparison of optimization results

	EGA	IGA (Choi and Yang, 2001)	SQP (Initial searching points: $x_1=0.5$, $x_2=1.0$)
$f(x_1, x_2)$	16.091720 16.091720 16.091720 16.091720	16.091713 16.091713 16.091051 16.091051	14.333086
Number of generation	26	10,000	
Computational time (s)	8.41	342.31	0.48

3. Application of Flexible Rotor System with SFD

3.1 Unbalance response and transmitted load

A typical SFD installed at an outer race of a ball bearing (inner damper element) supporting shaft is shown in Figure 3. The outer race is restrained from rotation by employing a soft centering spring shown in Figure 3. The centering spring is preloaded to offset any gravitational forces. Therefore, the shaft processes in a steady state in the circular concentric orbit about the fixed origin. When oil fills between the inner and outer elements of the damper, an oil film forms in the damper.

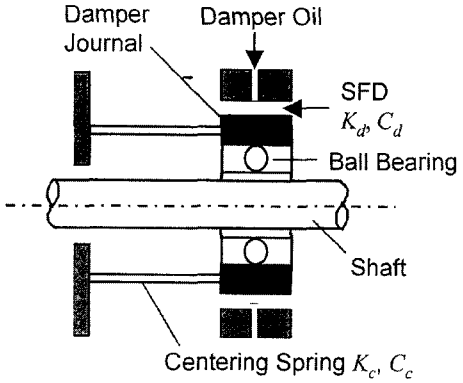

Fig. 3 Typical configuration of a SFD

When we used the short bearing approximation to model the SFD, assumed cavitation in the oil film (π film) and assumed circular synchronous motion for the rotor, the nonlinear equivalent stiffness K_d and damping coefficients C_d of the damper was represented by (Chen et al., 1988).

$$K_d=\frac{2\mu RL^3\Omega\varepsilon}{C^3(1-\varepsilon^2)^2},\quad C_d=\frac{\pi\mu RL^3}{2C^3(1-\varepsilon^2)^{3/2}} \tag{5}$$

where R, L and C are radius, length and radial clearance of the SFD, respectively. $\varepsilon(=e/C)$ is the damper eccentricity ratio. e is the displacement eccentricity of the damper journal. The governing equation for the unbalanced rotor system modeled by the finite element method (FEM) can be represented as

$$\boldsymbol{M}\ddot{\boldsymbol{p}}+\boldsymbol{D}\dot{\boldsymbol{p}}+\boldsymbol{K}\boldsymbol{p}=\boldsymbol{F} \tag{6}$$

where the matrices $\boldsymbol{M}$, $\boldsymbol{D}$, and $\boldsymbol{K}$ are the mass, damping and stiffness matrices, respectively. $\boldsymbol{p}$ and $\boldsymbol{F}$ in Eq. (6) are the steady-state displacement and unbalance force vectors, respectively. When the rotor system subjected to harmonic excitation is considered, $\boldsymbol{p}$ and $\boldsymbol{F}$ can be expressed as follows:

$$\boldsymbol{p}=\boldsymbol{p}_c\cos\Omega t+\boldsymbol{p}_s\sin\Omega t \tag{7}$$

$$\boldsymbol{F}=\boldsymbol{F}_c\cos\Omega t+\boldsymbol{F}_s\sin\Omega t \tag{8}$$

where Ω is the rotating speed and $\boldsymbol{p}_c$, $\boldsymbol{p}_s$, $\boldsymbol{F}_c$, and $\boldsymbol{F}_s$ are the displacement and force amplitudes components of cosine and sine terms. When Eqs. (7) and (8), and the first and second derivatives of Eq. (7) are substituted into Eq. (6), the cosine and sine components of the displacement vectors are obtained from

$$\begin{Bmatrix}\boldsymbol{p}_c\\ \boldsymbol{p}_s\end{Bmatrix}=\begin{bmatrix}\boldsymbol{K}-\Omega^2\boldsymbol{M} & \Omega\boldsymbol{D}\\ -\Omega\boldsymbol{D} & \boldsymbol{K}-\Omega^2\boldsymbol{M}\end{bmatrix}^{-1}\begin{Bmatrix}\boldsymbol{F}_c\\ \boldsymbol{F}_s\end{Bmatrix} \tag{9}$$

The magnitude of k-th node can be written as

$$p_k=\begin{bmatrix}p_{Zc\,k}\\ p_{Yc\,k}\end{bmatrix}\cos\Omega t+\begin{bmatrix}p_{Zs\,k}\\ p_{Ys\,k}\end{bmatrix}\sin\Omega t \tag{10}$$

where the subscript Z and Y are two perpendicular directions at the whirling plane. The damper displacement used in calculating the transmitted load can be obtained from the nonlinear Eq. (9) using an iterative solution scheme (Greenhill and Nelson, 1981) to determine the displacement eccentricities and the associated stiffness and damping coefficients. The problem is that the stiffness and damping coefficients in Eq. (5) are functions of the displacement eccentricity. When the displacement eccentricity in order to calculate the stiffness and damping coefficients could be first assumed, the assumed eccentricity must satisfy tolerances of the response amplitudes. The magnitude of the transmitted load TR through a typical support by the SFD shown in Figure 3 is given by,

$$TR=(TR_y^2+TR_z^2)^{1/2} \tag{11}$$

where

$$\begin{aligned}TR_y&=(K_d+K_c)\,y-\Omega(C_d+C_c)\,z=K_{dc}y-\Omega D_{dc}z\\ TR_z&=\Omega(C_d+C_c)\,y+(K_d+K_c)\,z=\Omega D_{dc}y+K_{dc}z\end{aligned} \tag{12}$$

In Eq. (12) z and y are the displacements in the Z and Y directions, and Eq. (12) from Eq. (10) can be replaced by

$$\begin{aligned}TR_y&=K_{dc}p_{Yc}-\Omega D_{dc}p_{Ys}\\ TR_z&=\Omega D_{dc}p_{Zc}+K_{dc}p_{Zs}\end{aligned} \tag{13}$$

3.2 Numerical example

Figure 4 shows the numerical model of a flexible rotor system supported by two SFDs as a numerical example, which is taken from Chen et al.(1988). The flexible rotor system modeled by the Timoshenko beam theory was analyzed by the FEM, and its unbalance response and transmitted load were also calculated in an operating speed range. This rotor is modeled as 13 stations (12 elements). Details of the rotor configurations and material properties are listed in Table 2. The rotor is supported on a rigid foundation by isotropic undamped bearings at stations 3, 6 and

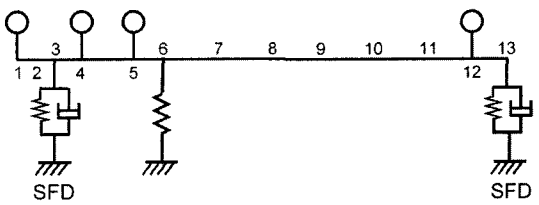

Fig. 4 Schematic diagram of a flexible rotor system with SFDs

13 with the spring properties listed in Table 3. The stiffness properties of the stations 3 and 13 represent those of the centering springs of the SFDs with the original design values listed in Table 4. The rotor includes four rigid discs located at stations 1, 4, 5 and 12 with mass properties listed in Table 5, and has the unbalance amount of 0.22 kg·mm at station 12. The operational speed range considered is from 100 rad/s to 2000 rad/s, which has the first two undamped forward critical speeds, 384.8 and 698.2 rad/s.

Table 2 Configuration data of a flexible rotor system

Element No.	Length (cm)	Inner radius (cm)	Outer radius (cm)
1	4.27	1.42	2.96
2	4.62	1.42	2.96
3	1.60	1.42	2.96
4	9.68	1.42	2.96
5	7.46	1.96	2.96
6	16.51	2.69	2.96
7	15.24	2.69	2.96
8	15.24	2.69	2.96
9	15.24	2.69	2.96
10	15.24	2.26	2.96
11	14.93	1.42	2.96
12	7.92	2.31	2.96
E=20.69 GN/m^2, ρ=8193.0 kg/m^3			

Table 3 Bearing stiffness data

Station No.	Stiffness (MN/m)
3	1.751
6	69.95
13	13.368

Table 4 Original SFD parameters

Length, L	25.4 mm
Radius, R	50.8 mm
Clearance, C	152.4 μm
Fluid viscosity	266×10^{-3} N·s/m^2

Table 5 Rigid disk data

Station No.	Mass (kg)	Polar moment of inertia (kg·cm$^2\times10^2$)	Transverse moment of inertia (kg·cm$^2\times10^2$)
1	11.38	19.53	9.82
4	7.88	16.70	8.35
5	7.70	17.61	8.80
12	21.70	44.48	22.24

4. Optimization of SFD

The rotor is supported in parallel by the two SFDs at stations 3 and 13. Thus, in this study, the object function is chosen as minmization of the maximum transmitted load TR_3 at station 3 and TR_{13} at the station 13 in the operational speed range. The unbalanced responses of the rotor system with the SFDs optimized by the EGA are compared with those of the original system and the system with the SFDs optimized by Chen et al.(1988). The SFD design prameters, the length L, radius R and radial clearance C are taken as the design varables as follows:

$$X=\{L\ R\ C\}^T \tag{14}$$

Even though the maximum transmitted load at station 13 was chosen as the objective function by Chen et al.(1988), the objective function in this study is fomulated as follows:

$$\begin{aligned}&\text{Find } X \text{ which minimizes the } max.\\ &f(X)=\alpha TR_3+\beta TR_{13}\end{aligned} \tag{15}$$

subject to

$$\left.\begin{aligned}&20.32\ \text{mm}\le L_{3,13}\le 30.48\ \text{mm}\\ &44.45\ \text{mm}\le R_{3,13}\le 57.15\ \text{mm}\\ &76.20\ \mu\text{m}\le C_{3,13}\le 254.0\ \mu\text{m}\end{aligned}\right\} \tag{16}$$

where subscripts 3 and 13 mean station 3 and 13. The maximum transmitted load of TR_3 is about 10 times smaller than that of TR_{13}, but the lower one, TR_3 is better for the stability of the rotor system than the higher one, TR_3. Therefore, the scale factors α and β were given as 10 and 1, respectively, to equalize the scales of TR_3 and TR_{13}.

Figure 5 shows the flow chart of the EGA for the optimal design of the nonlinear SFDs to the minimization of the maximum transmitted load

Table 6 Design parameters for the original and optimized SFDs and maximum transmitted loads

	Length (mm)		Radius (mm)		Clearance (μm)		Max. TR(N)/operating speed (rad/s)	
Station No.	3	13	3	13	3	13	3	13
Original	25.40	25.40	50.80	50.80	152.4	152.4	104.36/702	1576.9/702
Chen et al.	26.54	30.31	51.56	57.03	145.1	81.1	30.73/398	315.5/827
EGA	30.48	30.48	57.14	57.15	125.8	76.2	17.28/764	284.1/879

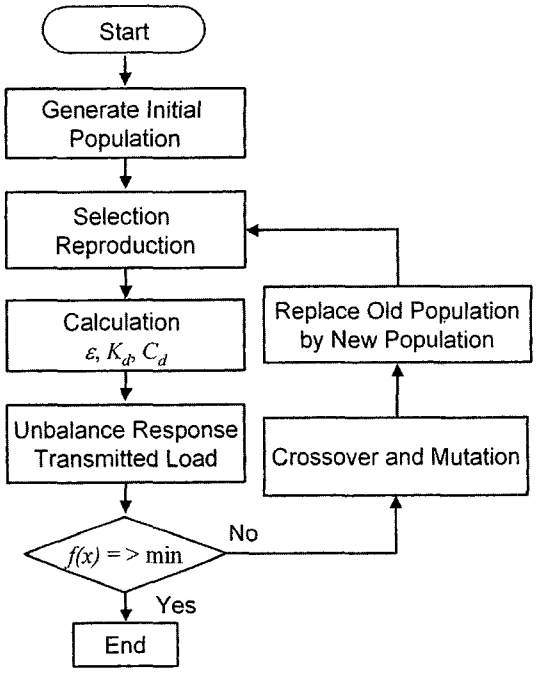

Fig. 5 Flow chart for the optimum design of the SFD by the EGA

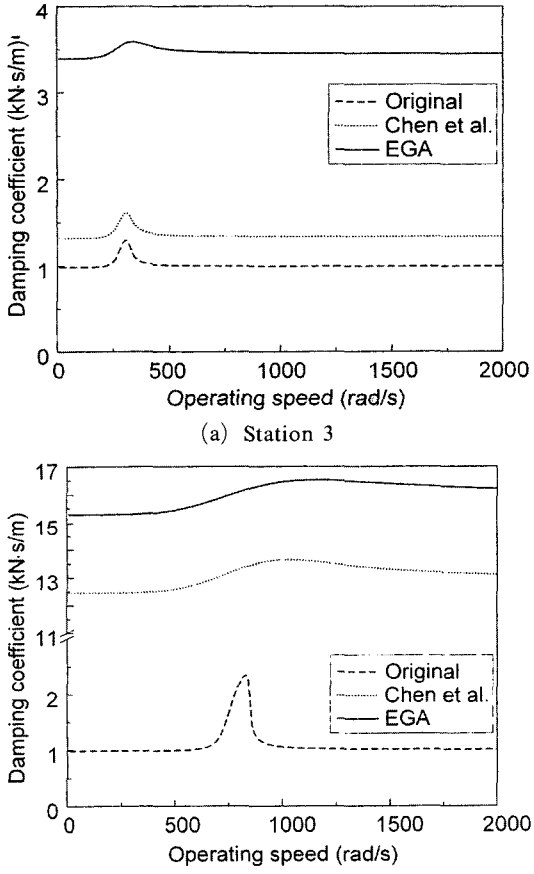

(a) Station 3

(b) Station 13

Fig. 6 Damping coefficients of SFDs

of the rotor system between the bearing and foundation in the operating speed range. In the first step, initial populations are created by using the genetic uniform distribution method and the variational mutation. In the following, the stiffness and damping coefficients and the eccentricity ratio of the SFDs supporting the masses of the rotor at stations 3 and 13 are calculated by each individual. After repeating the procedure until the assumed displacement eccentricity satisfies the criterion of convergence and evaluating the fitness of each individual, the position of the individuals with the highest fitness should be estimated as the optimum design value.

The design parameters of the SFDs optimized by Chen et al. (1988) and the EGA are compared with the original parameters in Table 6 and the maximum transmitted loads of the rotor with the SFDs optimized by them are compared with the original parameters. The values of the length and radius of the SFDs optimized by the EGA at stations 3 and 13 almost equal the upper limit of calculation boundaries. However, with changed limitation of the parameter boundaries, the EGA found different sets of design parameters. The damping and stiffness coefficients plots calculated

Table 7 Damping ratios at stations 3 and 13

	1st and 2nd critical speed ω(rad/s)	Station 3 (Mass: M_3=21.46 kg)			Station 13 (Mass: M_{13}=22.48 kg)		
		ξ_3	K_d (MN/m)	C_d (kN·s/m)	ξ_{13}	K_d (MN/m)	C_d (kN·s/m)
Original	387	0.361	0.0959	1.0351	0.886	0.0137	0.9839
	702	0.362	0.0886	0.9973	0.200	0.3944	1.1918
Chen et al.	398	0.416	0.1295	1.3861	2.329	0.3145	12.4856
	827	0.399	0.1310	1.3377	0.797	3.1328	13.3736
EGA	419	0.678	0.3178	3.5386	2.389	0.4593	15.3548
	879	0.565	0.4363	3.4582	0.884	3.9664	16.2721

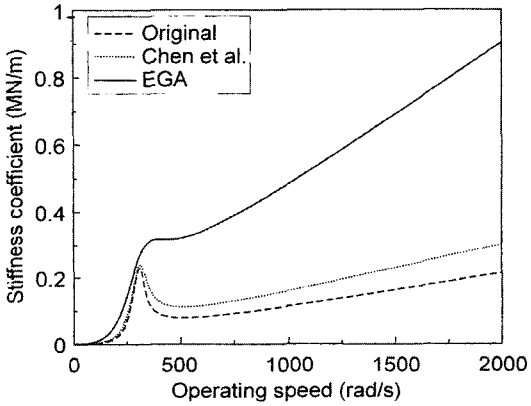

(a) Station 3

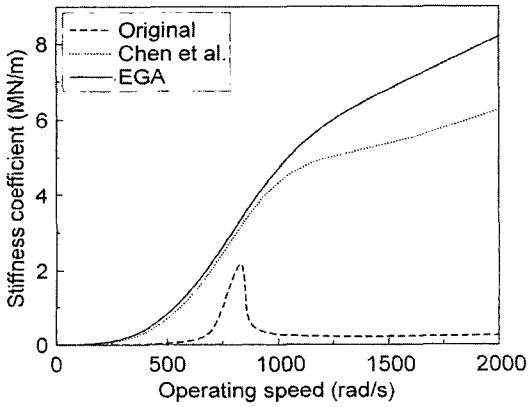

(b) Station 13

Fig. 7 Stiffness coefficients of SFDs

by using the design parameters listed in Table 6 are represented in Figures 6 and 7, respectively.

The damping coefficients for the three cases at station 3 shown in Figure 6 have maximum values in front of the first critical speed of the transmitted load, while the coefficients at station 13 have maximum values behind the second critical peed. The first and second critical speeds of the transmitted load are listed in Table 7. The characteristics of the stiffness coefficients of the SFDs are shown in Figure 7. After the stiffness coefficients at station 3 for the original design and Chen et al.(1988) increased and decreased greatly in front of the first critical speed, the coefficients repeatedly increased a little according to the increase in the operational speed. However, the coefficient for the EGA rapidly increased in front of the first critical speed and also increased greatly without decreasing according to the increase in the operating speed. The coefficients of the original design at station 13 increased and decreased greatly behind the second critical speed, and converged into a constant value, while the coefficients of Chen et al.(1988) and the EGA greatly increased from the first critical speed according to the increase in the operating speed. The damping coefficient has a stable value in the operational speed range, while the stiffness coefficients for all cases at station 3, for Chen et al.(1988) and the EGA at station 13 increase according to the increase in the operational speed.

Figure 8 represents the damping ratios obtained from the damping and stiffness coefficients of the SFDs and the mass of the rotor supported by the SFDs at stations 3 and 13. The damping ratios ξ_3 and ξ_{13} at stations 3 and 13 were defined as follow,

$$\xi_i = C_{di}/(2\sqrt{K_{di}M_i}) \quad (i=3,\ 13) \tag{17}$$

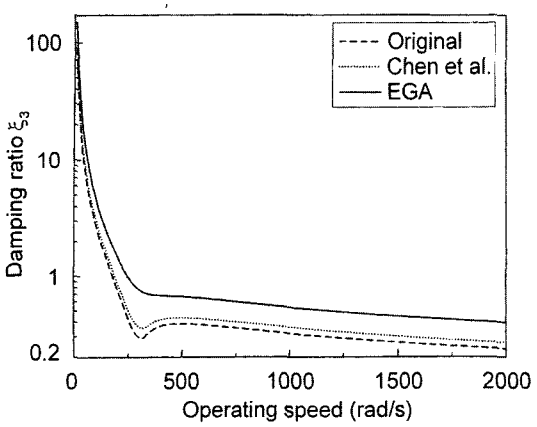

(a) Station 3

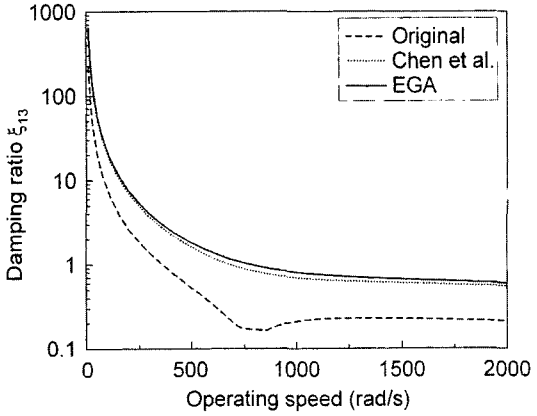

(b) Station 13

Fig. 8 Damping ratio at stations 3 and 13

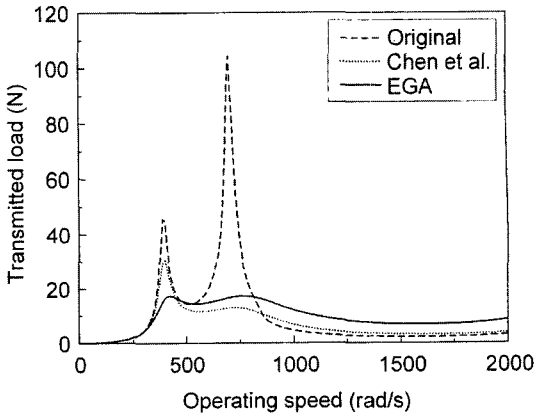

(a) Station 3

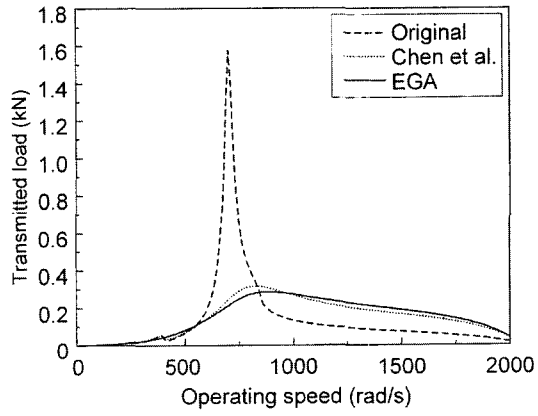

(b) Station 13

Fig. 9 Transmitted load in the operational speed range

The damping ratios of the EGA at each station are higher than those of the original design and Chen et al. (1988). The damping ratios of the first and second critical speeds at stations 3 and 13 are listed in Table 7.

The transmitted load plots of the rotor system with the SFDs which are the original design and optimized by Chen et al. (1988) and the EGA are shown in Figure 9. The plots show that the maximum transmitted load of the EGA is the lowest in the operating speed range and the values of the maximum transmitted load for three cases are listed in Table 6. The maximum transmitted load of the rotor system using the SFDs optimized by the EGA at station 13 has no great difference from that of the system using the SFDs optimized by Chen et al. (1988), while at station 3 there is a great difference. At station 13, the maximum transmitted load by the EGA reduced by about 82% in comparison with the original design and also by about 10% in comparison with Chen et al. (1988)'s design, while at station 3 it reduced by about 83% and also by about 44%. Why is the maximum transmitted load of the rotor system using the SFDs optimized by the EGA is lower than that of the system using the SFDs optimized by Chen et al. (1988). Since the search of the gradient-based NLP technique used by Chen et al. (1988) probably converged into an unstable solution according to the initial values of the design variables, the search could not find a global optimal solution. These results mean that global optimization techniques like the EGA are better than local optimization techniques like the NLP technique to optimize the design of the

nonlinear SFD.

5. Conclusions

The SQP which is well known as the NLP technique is more quickly converged into a solution than the EGA, IGA and a general GA, but is not able to find global optimum solutions according to an initial value because the NLP technique tends to converge into unstable solutions according to the initial design values. A general GA is also more quickly converged into a global optimum solution without converging to unstable solutions than the EGA, but it can not optimize multi-modal functions and solutions by the GA is not as accurate as that by the EGA. However, the optimization techniques offer a trade-off between running time and solution accuracy.

The EGA is a global optimization technique and is able to optimize multi-modal functions. The advantages of the EGA are less searching time and increased solution accuracy compared with the IGA. Furthermore, the EGA does not require sensitivity analysis and gradient of an objective function which are needed for conventional gradient-based optimization techniques.

The EGA is applied to the optimization of the nonlinear SFD by using design parameters to minimize the maximum transmitted load in the operational speed range. The maximum transmitted load of the rotor system with the SFD optimized by the EGA compared with the original design was greatly reduced, and the optimization results of the EGA are also better than those of the gradient-based NLP technique used by Chen et al.(1988) and especially better at station 3. From these results, it is considered that the EGA as a global optimization technique can be useful to optimize engineering problems.

References

Ahn, Y. K., Morishita, S. and Yang, B. S. 1998, "Directionally Controllable Squeeze Film Damper Using Liquid Crystal," *KSME International Journal*, Vol. 12, No. 6, pp. 1097~1103.

Chen, W. J., Rajan, M., Rajan, S. D. and Nelson, H. D., 1988, "The Optimal Design of Squeeze Film Dampers for Flexible Rotor System," *Trans. ASME Journal of Mechanisms, Transmissions, and Automation in Design*, Vol. 110, pp. 166~174.

Choi, B. G. and Yang, B. S., 2001, "Multi-objective Optimization of Rotor-Bearing System with Dynamic Constraints Using IGA Algorithm," *Trans. ASME Journal of Engineering for Gas Turbines and Power*, Vol. 123, No. 1, pp. 78~81.

Choi, B. G. and Yang, B. S., 2000, "Optimum Shape Design of Shaft Using Genetic Algorithm," *Journal of Vibration and Control*, Vol. 6, No. 2, pp. 207~222.

Cunningham, R. E., Fleming, D. P. and Gunter, E. J., 1975, "Design of a Squeeze Film Damper for a Multi-Mass Flexibler Rotor," *Trans. ASME Journal of Engineering for Industry*, Vol. 97, No. 4, pp. 1383~1389.

Davis, L., 1991, Handbook of Genetic Algorithms, Van Nostrand Reinhold, pp. 3~23.

De Jong, K. A., 1975, "An Analysis of the Behavior of a Class of Genetic Adaptive System," Doctoral Dissertation, *The University of Michigan, Ann Arbor, Michigan.*

De Santiago, O., San Andres, L. and Oliveras, 1999, "Imbalance Response of a Rotor Supported on Open-Ends Integral Squeeze Film Dampers," *Trans. ASME Journal of Gas Turbines and Power*, Vol. 121, No. 4, pp. 718~724.

Friswell, M. I. and Mottershead, J. E., 1996, "Finite Element Model Updating in Structural Dynamics," *Kluwer Academic Publishers*, Vol. 38, pp. 56~59.

Goldberg, D. E., 1989, *Genetic Algorithms in Search, Optimization & Machine Learning*, Addison-Wesley Publishing Company, pp. 1~146.

Greenhill, L. M. and Nelson, H. D., 1981, "Iterative Determination of Squeeze Film Damper Eccentricity for Flexible Rotor Systems," *Trans. ASME Journal of Mechanical Design*, Vol. 104, No. 2, pp. 334~338.

Gunter, E. J., Barrett, L. E. and Allaire, P. E., 1977, "Design of Nonlinear Squeeze-Film Dampers for Aircraft Engines," *Trans. ASME Journal*

of Lubrication Technology, Vol. 99, No. 1, pp. 57~64.

Hashimoto, H., 1997, "Optimum Design of High-Speed, Short Journal Bearings by Mathematical Programming," *Tribology Transactions*, Vol. 40, pp. 283~293.

Lin, Y., Cheng, L. and Huang, T. P., 1998, "Optimal Design of Complex Flexible Rotor-Support Using Minimum Strain Energy Under Multi-Constraint Conditions," *Journal of Sound and Vibration*, Vol. 215, No. 5, pp. 1121~1134.

Lubell, D. and San Andres, L., 1998, "Imbalance Response of a Test Rotor Supported on Squeeze Film Dampers," *ASME Journal of Engineering for Gas Turbines and Power*, Vol. 120, No. 2, pp. 397~404.

Kim, Y. C., Choi, S. P., Yang, B. S. and Lee, S. J., 2001, "Enhanced Genetic Algorithm for Fast and Accurate Global and Local Optimization Search," *Proceedings of 8th International Congress on Sound and Vibration*, July 2-6, Hong Kong, pp. 2143~2150.

Merz, P. and Freisleben, B., 2000, "Fitness Landscape Analysis and Mimetic Algorithms for Quadratic Assignment Problem," *IEEE Trans. on Evolutionary Computation*, Vol. 4, No. 4, pp. 337~352.

Mohan, S. and Hahn, E. J., 1974, "Design of Squeeze Film Damper Supports for Rigid Rotors," *Trans. ASME Journal of Engineering for Industry*, Vol. 96, No. 3, pp. 976~982.

Nelder, J. A. and Mead, R., 1965, "A Simplex Method for Function Minimization," *Computer Journal*, Vol. 7, pp. 308~313.

Okamoto, M., Nonaka, T., Ochiai, S. and Tominaga, D., 1998, "Nonlinear Numerical Optimization with Use of a Hybrid Genetic Algorithm Incorporated the Modified Powell Method," *Applied Mathematics and Computation*, Vol. 91, pp. 63~72.

Rabinowitz, M. D. and Hahn, E. J., 1983, "Optimal Design of Squeeze Film Supports for Flexible Rotors," *Trans. ASME Journal of Engineering for Power*, Vol. 105, pp. 487~494.

Sato, T. and Hagiwara, M., 1998, "Bee System : Finding Solution by a Concentrated Search," *Trans. IEE Japan*, Vol. 118-C, No. 5, pp. 721~726.

Satio, S. and Kobayashi, M., 1982, "On the Vibration of a Rotor Supported by Squeeze Film Damper," *Trans of the Japan Society of Mechanical Engineers, Series C*, Vol. 48, No. 436, pp. 1883~1888.

Shiau, T. N., Hwang, J. L. and Chang, Y. B., 1993, "A Study on Stability and Response Analysis of a Nonlinear Rotor System With Mass Unbalance and Side Load," *Trans. ASME Journal of Engineering for Gas Turbines and Power*, Vol. 115, pp. 218~226.

Thomsen, K. K. and Andersen, H., 1974, "Experimental Investigation of a Simple Squeeze Film Damper," *Trans. ASME Journal of Engineering for Industry*, Vol. 96, No. 2, pp. 427~430.

The Mathworks Inc. *Optimization Toolbox for Use with Matlab*, Version 2. i (Release 12).